Self-assembling protein platform for direct quantification of circulating microRNAs in serum with total internal reflection fluorescence microscopy

Ho, See-Lok; Chan, Ho-Man; Wong, Ricky Ngok-Shun; Li, Hung-Wing

Published in:
Analytica Chimica Acta

DOI:
10.1016/j.aca.2014.03.020

Published: 01/05/2014

Document Version:
Peer reviewed version

Self-assembling Protein Platform for Direct Quantification of Circulating MicroRNAs at Femtomolar level in Serum with Total Internal Reflection Fluorescence Microscopy

See-Lok Ho[a], *Ho-Man Chan*[a], *Ricky Ngok-Shun Wong*[b,*], *Hung-Wing Li*[a,*]

[a]Department of Chemistry and [b]Department of Biology, Hong Kong Baptist University, Kowloon Tong, Hong Kong, P.R. China

[*]Corresponding author. *Email address:* hwli@hkbu.edu.hk (H.W.Li), rnswong@hkbu.edu.hk (R.N.S.Wong)

ABSTRACT

MicroRNA (miRNA) has recently emerged as a new and important class of cellular regulators. Strong evidences showed that aberrant expression of miRNA is associated with a broad spectrum of human diseases, such as cancer, diabetes, cardiovascular and psychological disorders. However, the short length and low abundance of miRNA place great challenges for conventional techniques in the miRNA quantification and expression profiling. Here, we report a direct, specific and highly sensitive yet simple detection assay for miRNA without sample amplification. A self-assembled protein nanofibril acted as an online pre-concentrating sensor to detect the target miRNA. Locked nucleic acid (LNA) of complimentary sequence was served as the probe to capture the target miRNA analyte. The quantification was achieved by the fluorescence intensity measured with total internal reflection fluorescence microscopy. A detection limit of 500 fM was achieved with trace amount of sample consumption. This assay showed efficient single-base mismatch discrimination. The applicability of quantifying circulating mir-196a in both normal and cancer patient's serums was also demonstrated.

1. Introduction

MicroRNAs (miRNAs) are non-coding RNAs of ~ 18-25 nucleotides. They initially exist in the cell nucleus as a long primary transcript, primary miRNAs (pri-miRNAs). By enzymatic cleavages of pri-miRNA and precursor miRNAs, mature miRNAs are produced. Mature miRNAs are found to be an important gene expression regulator, which are involved in early tumorgenesis and tumor progression[1-3]. Abnormal and distinctive expression profile of miRNAs is found in different types of tumor tissues and cancers. miRNAs expression profiling is therefore regarded as an important biomarker for cancer diagnosis[4-5].

Meanwhile, circulating miRNAs in body fluids, such as serum, blood plasma and urine, are found to be well-preserved and highly correlated to pathological changes. These endogenous miRNAs are highly stable in a range of temperature and pH and they are robust against RNase digestion[6-7]. Although the mechanism behind the high resistance of circulating miRNA against degradation is still not well-understood, researchers proposed that the circulating miRNAs are protected by the RNA-induce silencing complex (RISC), which forms an extra protection towards the fragile miRNAs[8]. With the potential that circulating miRNAs can be collected non-invasively in serum, plasma, and urine, circulating miRNAs are considered as a potential biomarker for clinical cancer diagnosis.

Since the level of circulating miRNAs is much lower (~ 20 pM)[9] compared to those in tissue and cells, a method of high sensitivity, specificity and high quantitative accuracy is very critical for a reliable miRNAs expression profiling. However, it is always challenging to determine directly and accurately the amount of miRNAs for their short length and low abundance. The short sequence limited the design of complementary

probe used to capture the target miRNAs and confined the mismatch discrimination efficiency. Quantitative reverse transcript PCR (qRT-PCR)[10], northern blotting[11], and microarray[12] are currently the golden methods to perform miRNAs expression profiling, although these methods encounter complications like sample loss during the amplification steps, large sample consumption, use of radioactive reagents, intensive labor and long assay time. As a result, other sample pretreatment strategies aiming at higher detection sensitivity, specificity, and minute sample consumption have been developed recently, for example, electrochemical[13-14], isothermal strand-displacement[15], and enzymatic amplification[16] detection assays. Taking advantage of the signal amplification technique, some of these detection assays are capable of quantifying miRNAs at attomolar level. However, the reliability and reproducibility of the assay are scarified by multiple manipulation and transversal steps. Our group previously reported a direct miRNA detection method by single-molecule counting with total internal reflection fluorescence microscopy (TIRFM)[17]. The miRNA detection assay is free of sample pre-treatment and amplification. The detection was achieved by counting the fluorescent analytes within the evanescent field layer in single-molecule level.

Over the recent decade, bio-sensing platform constructed from different novel nanomaterials has been widely applied for detection of biomolecules like DNAs, miRNAs proteins etc. Thaxton *et.al* developed a sensitive scanometric miRNA detection assay using gold nanoparticles[18]. Other nanomaterials such as silver nanowires[19], silicon nanowires[20], and tin dioxide[21], have also been incorporated into the detection assays. The resulted signal enhancement dramatically improves the sensitivity of the detection assay, shortens the assay time, and reduces the sample consumption by pre-concentrating the

analytes on the surface of the nanocomposites. However, most of the nanoparticles are limited to the working conditions such as solution pH and ionic strength, possibly resulting in self-aggregation and activity loss. Unlike the fabrication of nanoparticles and nanowires which requires sequential chemical synthetic techniques, self-assembled bionanocomposite with peptides simultaneously forms a well-structured, well-defined and stable macromolecular structure[22]. Having peptides as the building blocks, the protein scaffold is inherently stable and of high activity under physiological conditions. Most importantly, the specificity and functionality of the protein scaffold can be manipulated by simply modifying the functional moiety of the protein motif. Amyloid fibril is well-known to be rich in β-sheet structure, which is rigid and stiff compared to other natural protein-based material like collagen and silk. Functionalized $A\beta_{1-40}$ fibril can be straightly obtained by co-incubating functionalized $A\beta_{1-40}$ monomer with native $A\beta_{1-40}$ monomer. It is demonstrated that the functionalized $A\beta_{1-40}$ fibril is of high potential to serve as biocompatible and highly stable pre-concentrating scaffold for biomarker detection.

Our group previously developed a functionalized self-assembling beta-amyloid (1- 40) ($A\beta_{1-40}$) fibril as a platform for biomolecules detection[23]. However, the hybridization efficiency of the surface-based assay is highly limited by diffusion kinetic of the analyte molecules. Here, we developed a solution-based direct miRNAs detection assay with self-assembling $A\beta_{1-40}$ fibril with TIRFM. As a proof-of-concept, hsa-mir-196a (mir-196a) was chosen to be the miRNA target for detection. Mir-196a was found to be one of the significant miRNAs elevated in nasopharyngeal[24], gastrointestinal[25], and pancreas[26] cancers. In the assay, self-assembling $A\beta_{1-40}$ fibrils were labeled with a mixture of Alexa

Fluor-555 streptavidin (AF 555 stv) and bare streptavidin (stv), to locate the fibrils. The target miRNAs were pre-hybridized with the complementary 5' biotinylated locked nucleic acid (LNA) probe in solution to achieve high hybridization efficiency and then labeled with fluorescent dye YOYO-1. The hybrid complexes were then added to the AF 555 stv-labeled $A\beta_{1\text{-}40}$ fibril, and were captured onto the backbone of the fibrils through the biotin and streptavidin interaction. The fluorescent images of fibril were collected by TIRFM. The target miRNAs was quantified with the fluorescent intensity of individual fibrils. This assay provided a limit of detection (LOD) at around 500 fM, as well as a high specificity as it substantially discriminated the two miRNAs within the same family, target mir-196a and mir-196b, which differ by a single nucleotide. The developed assay was applicable for the direct determination of the mir-196a concentration in both normal and cancer patient's serum samples without sample pre-treatment. This direct, sensitive and specific detection assay for miRNAs is of high potential for clinical application for early stage cancer diagnosis.

2. Material and methods

2.1 Coverslides pretreatment. All the coverslides were prewashed prior to use. Generally, No.1 22 × 22 mm square glass (Menzel-Glaser, Germany) were successively sonicated for 15 min in household detergent, 15 min in absolute ethanol, 40 min in 1 M sodium hydroxide, 15 min in acetic acid, then 5 min in absolute ethanol thrice. The coverslides were rinsed thoroughly with filtered distilled water between every solvent replacement. The cleaned coverslides were dried in the oven at 120 °C for 3 hrs and stored for further use.

2.2 Preparation of $A\beta_{1-40}$ Fibrils for seeding. Monomeric $A\beta_{1-40}$ was purchased from Invitrogen and used without further purification. The stock $A\beta_{1-40}$ monomer solution was prepared by dissolving 0.1 mg $A\beta_{1-40}$ monomer with 400 µL 0.02 % ice-cold ammonia solution and stored at – 20 °C until use. The seed was prepared as mentioned elsewhere[27-29]. Briefly, by diluting the stock $A\beta_{1-40}$ monomer to 57.7 µM with 1× phosphate buffer (50 mM sodium phosphate, pH 7.4); the solution was incubated at 37 °C for 20 hrs under gentle shaking. The second generation of $A\beta_{1-40}$ seeding was prepared by adding 1 µL of 0.87 µg/mL $A\beta_{1-40}$ seeding from the previous step to 2 µL of $A\beta_{1-40}$ monomer and diluted to 20 µL with 1× phosphate buffer. The solution mixture was incubated at 37 °C for 1 hr. The resultant fibrils were used as the second generation of seeding for further fibrillation.

2.3 Preparation of Biotinylated $A\beta_{1-40}$ Fibrils. The stock biotin functionalized $A\beta_{1-40}$ monomer (Anaspec, USA) was diluted with 0.02 % ice-cold ammonia solution to 100 µM. The biotinylated $A\beta_{1-40}$ fibrils were prepared by incubating 20 % of biotinylated $A\beta_{1-40}$ monomer with native $A\beta_{1-40}$ monomer in 0.5× phosphate buffer. The total concentration of the $A\beta_{1-40}$ monomer is 50 µM. In order to accelerate the fibrillation process, 1 µL of 0.87 µg/ mL $A\beta_{1-40}$ seeding was added to the solution. The fibrils were diluted to 200-fold with phosphate buffer prior to experiments.

2.4 Preparation of Hybridization Buffer. The 1× Tris-EDTA buffer with 250 mM NaCl (TNE 250) was prepared by mixing 20 mM pH 8.0 Tris-HCl (Invitrogen, Carlsbad, CA) with 1 mM EDTA (Sigma-Aldrich) and 250 mM sodium chloride in distilled water. The pH of the buffer was adjusted to pH 7.4 with 2 M HCl. The buffer was filtered through a 0.2 µm nylon membrane filter and autoclaved prior to use.

2.5 Preparation of Probes and Target MicroRNA Oligonucleotides. The commercial available LNA-modified oligonucleotide probes (miRCURY LNA™ microRNA Detection Probes) LNA196a (5'-CCCAACAACATGAAACTACCTA-3') specific to corresponding target microRNAs was purchased from Exiqon (Denmark). The HPLC-purified synthetic mature microRNA oligonucleotides *hsa-mir-149* (5'-UCUGGCUCCGUGUCUUCACUCCC-3'), *hsa-mir-196a* (5'-biotin-UAGGUAGUUUCAUGUUGUUGGG-3') and *hsa-mir-196b* (5'-UAGGUAGUUUCCUGUUGUUGGG-3') were custom synthesized and purchased from Integrated DNA Technology (USA), acting as the target microRNA strands. All oligonucleotides were suspended in 500 μL DEPC-treated water (Ambion, USA) and diluted to appropriate concentration with 1× TNE 250 buffer.

2.6 Study of the hybridization efficiency. Sealed flow cell channel was prepared by combining prewashed coverslides with double-sided adhesive tape. Each channel is around 3 mm wide. For detection, 10 μL of the diluted $A\beta_{1\text{-}40}$ fibrils was first flowed into the channel; followed by adding excess stv/ AF 555-Stv mixture (molar ratio of 2:1). The channels were successively washed with phosphate buffer between each consecutive sample addition. In the study of the hybridization efficiency, surface base hybridization duplex was prepared as reported previously[23]. Briefly, excess poly $(T)_{15}$ probe (5'-biotin-TTT TTT TTT TTT TTT-3', Invitrogen, HPLC-purified) was added to the channel that contained the stv/ AF 555-stv labeled fibril and incubated for 15 min. Then 50 pM poly $(A)_{15}$ target (5'-AAA AAA AAA AAA AAA-3', Invitrogen, HPLC-purified) was flowed into the channel and hybridized for 30 min. Finally, fluorescent dye YOYO-1 was added

to label the hybrids for further quantification by TIRFM. The ratio of the YOYO-1 and the hybridized base pair was 1:3 (dye/ bp).

The solution-based hybridization duplex was prepared by hybridization 500 pM poly $(A)_{15}$ with 500 pM biotinylated poly $(T)_{15}$ probe in solution at room temperature for 30 min and fluorescent dye YOYO-1 was added to label the hybrids. The ratio of the YOYO-1 and the hybridized base pair was 1:3 (dye/ bp). The hybrids were then added into the channel with the AF 555-stv labeled fibril as mentioned in the previous step and incubated for 1 hr to saturate the streptavidin site and for further detection by TIRFM. Three experimental trials were performed, while the mean of mean and standard error of the mean from the triplicates were taken to the plot unless specified.

2.7 Hybridization of the MicroRNAs. All the LNA probes and miRNA strands were diluted to 1 nM with 1× TNE 250 buffer (pH 7.4), respectively. The hybridization cocktail contained target miRNA strand at different concentrations (0, 0.5, 1, 5, 10, 25, 50, 100 pM respectively), 100 pM corresponding LNA probe and hybridization buffer. The solution mixture was incubated in heating block (Labnet, USA) for 1 hr. The hybridization temperature was set to 20 °C below the melting temperature (*Tm*) of the LNA probe, which is 58 °C. The *Tm* was predicted based on the thermodynamic nearest neighbor method[30].

2.8 Labeling of MicroRNAs. After incubation, YOYO-1 was added to label the hybrids (biotinylated-LNA-miRNA duplex). The ratio of the YOYO-1 and the hybridized base pair was 1:3 (dye/ bp). The YOYO-1 labeled hybrids were incubated in room temperature for 5 min for equilibrium.

2.9 Quantification of mir-196a with $A\beta_{1-40}$ fibrils on the surface of the flow cell. Different concentrations of target microRNAs hybrid (0, 0.5, 1, 5, 10, 25, 50, and 100 pM respectively) were added into each of the channels that contained the stv/ AF 555-stv labeled fibril and incubated for 30 min for further quantification.

For the mismatch study, 50 pM hsa-mir-196b and hsa-mir-149 hybrids were used to show the specificity of the assay. The fluorescent images of the fibrils detection platform were captured under a home-built total internal reflection fluorescence microscopy system (TIRFM) with an excitation 488 nm cyan laser (50 mW, CMA1-01983, Newport, USA).

2.10 Quantification of mir-196a in serum samples by TIRFM. Serum samples were obtained from the Nasopharyngeal Carcinoma Area of Excellence Research Tissue Bank under the Center for Nasopharyngeal Carcinoma Research, the serum samples were stored at -80 °C prior to use without further modification. Synthetic mir-196a, with a final concentration of 0, 1, 2, 5, 10, and 15 pM respectively, was spiked into the standard addition cocktail which contained 3.5 µL of the 5-fold diluted serum and LNA probe of a final concentration of 100 pM, and finally diluted to 20 µL with TNE buffer. The solution was incubated at 58 °C for 1 hr. Finally, the quantification was constructed as mentioned above.

2.11 Fluorescence imaging and data analysis. The prism type total internal reflection fluorescence microscopy was setup as mentioned before[17, 23]. Briefly, the flow cell was placed between a fused-silica isosceles prism (CVI, laser USA) and a 60× oil type objective equipped with an Olympus IX71 inverted microscopy with a HQ 535/50 (Chroma) band-pass filter. A 488-nm diode laser (Newport, USA) was used as the

excitation source to excite the YOYO-1 dye. The fluorescence image of the $A\beta_{1-40}$ fibrils was captured by an Electron Multiplying Charge Coupled Device (EMCCD) (PhotonMax 512, Princeton Instrument, USA) incorporated with a Uniphase mechanical shutter (Model LS2Z2, Vincent Associates, USA) and a driver (Model VMM-T1, Vincent Associates, USA) in external synchronization and frame-transfer mode. The exposure time of both camera and shutter were set at 100 ms. The multiplication gain and the delay time of the shutter drive were set at 4000 and 10 ms respectively. The fluorescence signal of the fibrils was measured by the free-domain software *Image J*. The fluorescence signals of the sensor was obtained by measuring net fluorescence intensity of 50 independent fibrils, which located randomly, in each condition with *Image J* (Region of interest = 15 × 2 square pixels). Net intensity = 50 × (15 × 2 square pixels of independent fluorescent area on fibrils) – 50 × (15 × 2 square pixels of independent background area on image). Three experimental trials were performed, while the mean of mean and standard error of the mean from the triplicates were used in the plot unless specified.

3. Results and discussions

3.1 Study of the hybridization efficiency. The quantification of the target oligonucleotide presented here is a hybridization-based assay. The hybridization efficiency of the target and the complimentary sequence is very crucial for the overall performance of the assay. We firstly compared the hybridization efficiency of the target oligonucleotide and the complimentary probes where hybridization occurs in solution and on surface. Figure 1 shows the net fluorescence intensity measured on the fibril loaded with 500 pM solution-based and surface-based hybridized poly $(A)_{15}$ and poly $(T)_{15}$ complex. Under the same concentration of the target and the probe, higher hybridization

efficiency is indicated by a higher detected fluorescence signal. The average fluorescence intensity of the fibrils loaded with solution-based hybridized complex was almost tripled over the surface-based one. This result suggested that solution-based hybridization was more efficient than surface-based. In surface-based hybridization, the detection probes were first immobilized on the backbone of the fibrils. Then the target single-stranded oligonucleotide reached the probes solely by diffusion. The overall hybridization rate is limited by the diffusion kinetic of the target analyte, the electrostatic repulsion of both negatively charged probes and targets, density of the surface-immobilized probe, probe immobilization efficiency and the steric hindrance. On the other hand, in solution-based hybridization, both the probe and the target are free in solution, the charge density is diluted due to large diffusion volume and, therefore they are subject to higher chance to interact and form hybrid. Comparing under the same hybridization time, solution-based hybridization offers higher efficiency. Therefore, solution-based hybridization was adopted for the miRNA detection assay in the following work.

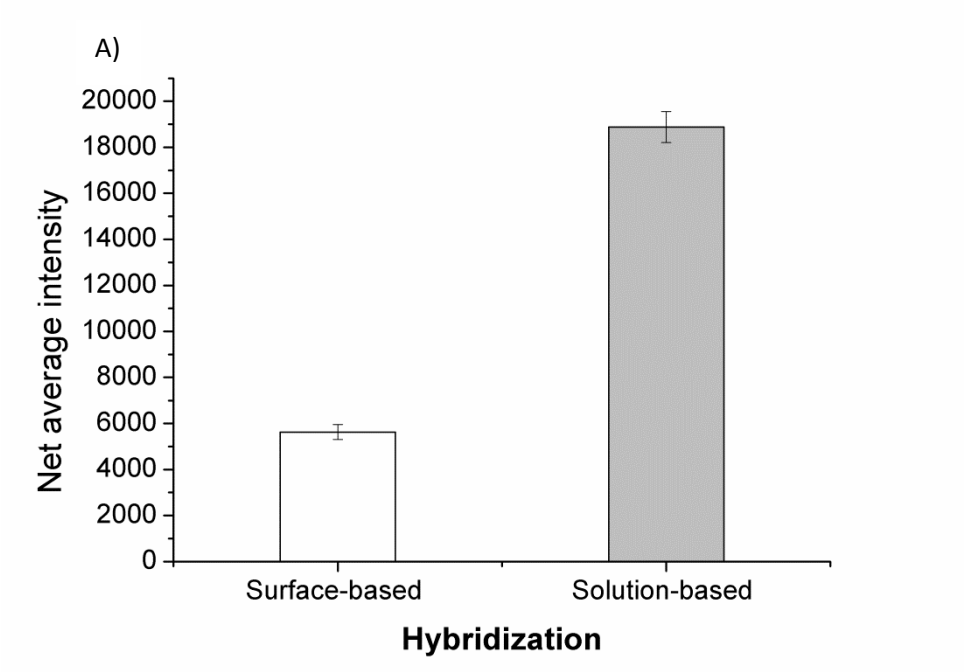

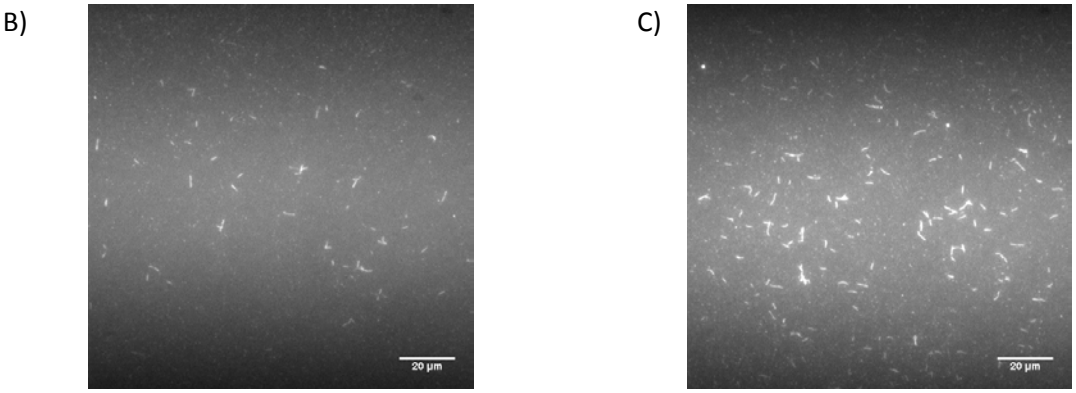

Figure 1. A) The average of resulted fluorescence signal on individual biosensing fibril, as an indication of the hybridization efficiency, obtained by solution-based and the surface-based hybridization with 500 pM poly A and complementary poly T probe. Error bar, standard error of mean. n = 3. (Net intensity = 50 × (15 × 2 square pixels of independent fluorescent area on fibrils) – 50 × (15 × 2 square pixels of independent

255 background area on image).) The fluorescence images of the fibrillar sensors detecting
256 poly A/poly T duplex duplexes formed by (B) surface-based hybridization; and (C)
257 solution-based hybridization. The hybridization efficiency of solution-based is
258 significantly higher than that of surface-based.

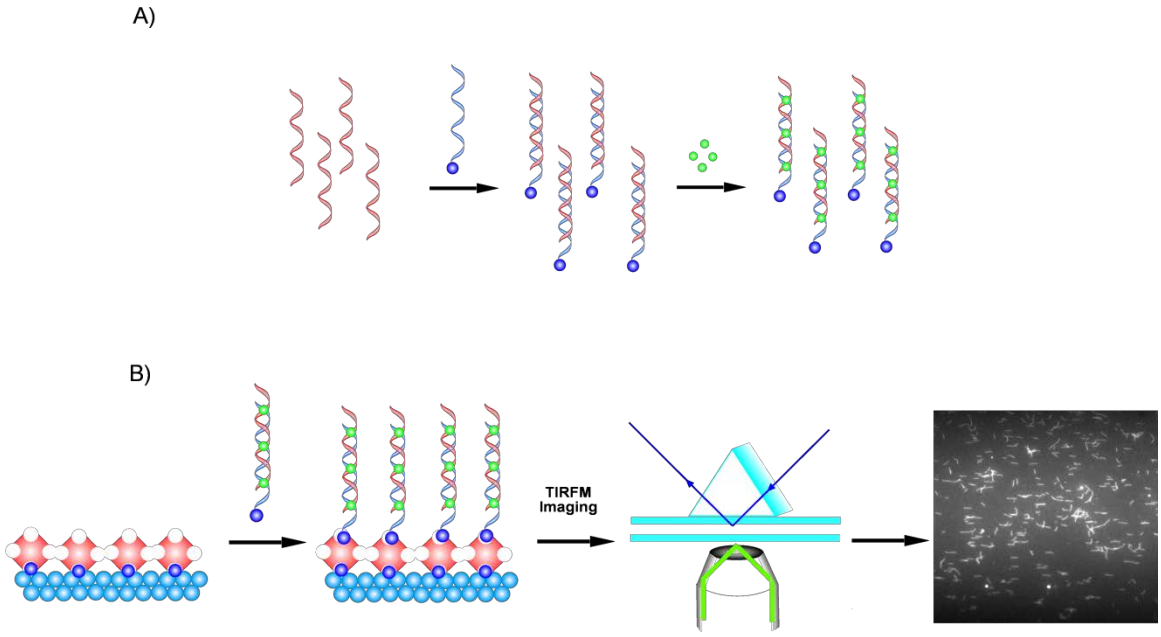

Figure 2. Schematics of the direct quantification of miRNA with a self-assembling protein fibrillar platform. (A) A hybridization-based detection for mir-196a by using biotin functionalized LNA196a detection probe. The hybrids were labeled with fluorescent dye YOYO-1. (B) The hybrids were then conjugated onto the surface of the amyloid protein fibril by biotin/streptavidin interaction for fluorescence measurement and quantification.

3.2 Detection assay. As a proof-of-concept, mir-196a was chosen as the target miRNA in this study. LNA modified nucleotide detection probe (LNA196a) with a biotin functionalized 5' terminal was designed. The target and the LNA probes were mixed and allowed for sufficient hybridization. The hybrids were then labeled with an intercalating fluorescent dye YOYO-1. The binding affinity of the YOYO-1 dye towards the double-stranded nucleic acid is around 6×10^8 M^{-1} with a fluorescence intensity enhancement of ~ 400-fold upon binding as compared to single-stranded.[31] The resulted fluorescence signal is employed for quantitative analysis.

The principle of the detection assay is illustrated in figure 2. Biotinylated fibrils were prepared by simply mixing and incubating the biotinylated amyloid monomer and native amyloid monomer for an hour. Each of the as-formed protein fibril acted as an individual platform for target analyte capturing. With the wide-view fluorescence imaging of large number of fibrils simultaneously, a detection of high-throughput was accomplished. We made use of the electrostatic and hydrophobic interaction between the protein fibrils and the glass slide surface that the fibrils could be immobilized and stretched upon capillary force once the fibrils were flowed into the channel which was comprised by two glass coverslides and adhesive tape. Neither pretreatment of the glass surface nor chemical modifications on the protein scaffold was required. As shown from the fluorescence images, the fibrils were consistently well-stretched and physically adsorbed on glass surface. After that, freely diffusing hybrids will then be captured onto the nanofibrils. Fluorescence signal from the labeled hybrids was collected for analysis. According to our previous study[23], the sensitivity of the detection assay was influenced by the density (or concentration) of $A\beta_{1-40}$ fibrils on the coverslide and the compositional percentage of the

biotin moiety on the fibrillar protein. As reported, the fibrils obtained by co-incubation of native monomer with 20 % of biotinylated $A\beta_{1-40}$ monomer gave optimal experimental conditions for the strongest fluorescence signal and therefore it was adapted in this current study. After the immobilization of the fibrils on the glass surface, the solution mixture of excessive stv/AF 555-stv was injected into the home-made channel to capture the biotinylated target hybrids as well as to label and locate the fibrils. It was found that the highly negative double-stranded hybrid did not have substantial non-specific adsorption onto the negative surface of the coverslides (at pH 7.4). Addition of the blocking agent, for example, BSA, was therefore not necessary (See figure S1).

As one of the wide-view fluorescence imaging techniques, TIRFM is regarded as a sensitive and powerful one to monitor chemical and biological systems at the glass/water interface. The fact that only the fluorophores (the immobilized protein fibrils with captured targets in this work) within the evanescent field layer was excited and hence high signal-to-noise ratio was provided. The set-up of the TIRFM system is shown in figure S2. A 488 nm laser was used to excite the YOYO-1 dye on the hybrids and the AF555 stv on the fibril. The angle of incidence of the laser beam is ~ 66 °, the total internal reflection occurred at the glass/solution interface and the penetration depth of evanescent field layer (d) was calculated to be 190 nm by $(d = \lambda / 4\pi(n_1)^2 sin^2\theta - n_2{}^2)^{1/2})$ where λ is the wavelength of the excitation source, n_1 and n_2 are the refraction indices of the solution and glass-surface, and θ is the angle of incidence. The fluorescence image of the fibrils was captured by the EMCCD.

To illustrate the performance of the developed miRNA assay, the LNA196a-mir-196a hybrids with different concentration of miRNA target (0 to 100 pM) were added to the

channel and captured on the surface of the fibrils through the strong biotin and streptavidin interaction. Individual fibrils loaded with hybridization complex of 0 to 100 pM mir-196a with 100 pM LNA196a were visualized under the TIRFM imaging system and the intensity was analyzed. A calibration curve of the fluorescence intensity collected as a function of the target concentration was constructed as shown in figure 3. A good linearity with a coefficient of determination of 0.994 was obtained. The limit of detection (LOD) of 500 fM was achieved (*LOD = mean of the blank + 3 × standard error of mean of blank*) for miR196a. As literature reported, the level of miRNAs in the cancer patient's serum sample is around 20 pM[9]. This as-developed assay is applicable to quantify the level of miRNAs in serum sample.

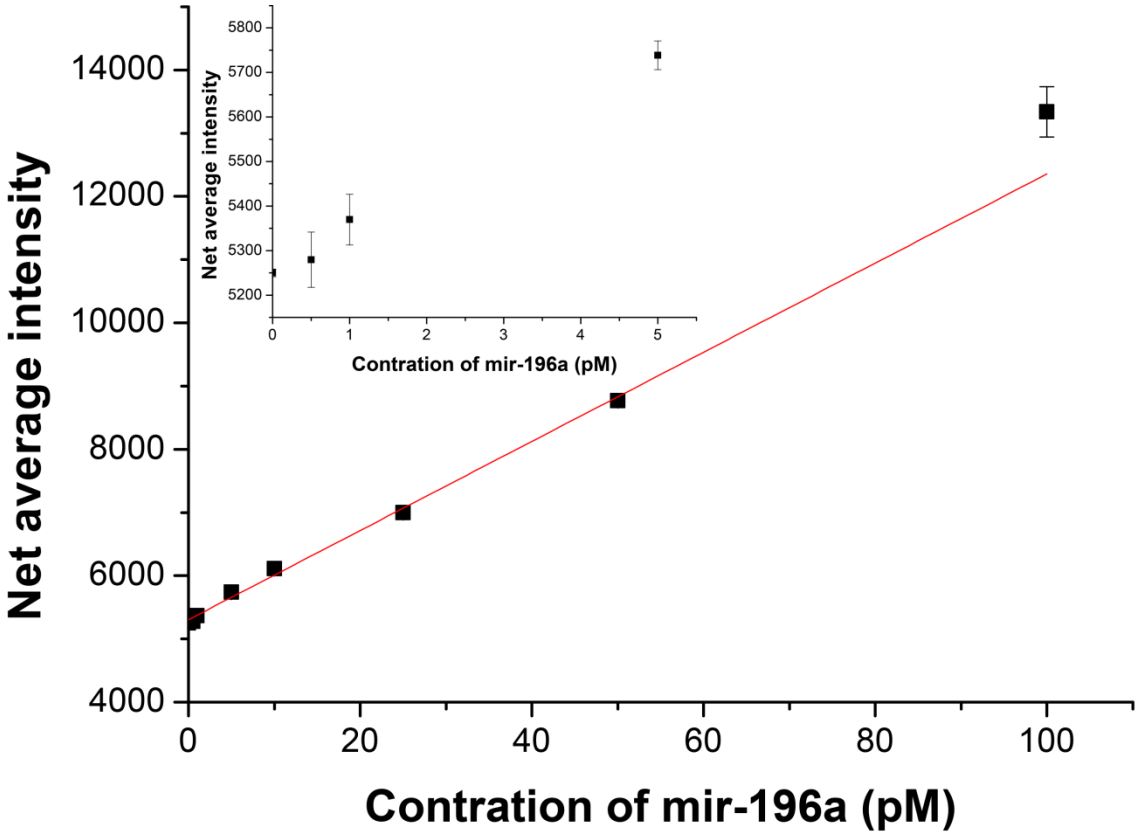

323

324 **Figure 3.** Calibration plot showing the linear relationship between net averaged
325 fluorescence intensity generated from the YOYO-intercalated miRNA hybrids and the
326 concentration of mir-196a, R^2= 0.994. Detection limit of the detection assay is 500 fM.
327 Error bars, standard error of mean, n = 3. (Net intensity = 50 × (15 × 2 square pixels of
328 independent fluorescent area on fibrils) – 50 × (15 × 2 square pixels of independent
329 background area on image).)

3.3 Specificity study. The sequences of the miRNAs within a family are very similar and some of them differ only by a single nucleotide. This places another challenge to obtain an accurate expression profiling of miRNAs from the same family. To demonstrate the specificity of this detection assay, mir-196b and a non-complementary miRNA (mir-149) were chosen. Literature reported that mir-149 also plays an important role in the development of nasopharyngeal carcinoma (NPC)[32]. Mir-196b is a family member of the mir-196 family, the optimal hybridization temperatures of the two miRNAs, mir-196a and mir-196b, differ by 2 °C. In the recent decade, locked nucleic acid (LNA) has been used as detection probe for a variety of miRNAs assay for significant increase in the sensitivity and specificity of the detection probe compared to using RNA and DNA probes. The methylene bridge connecting the 2'O and the 4'C of the ribose backbone fixed the LNA modified nucleotide such that the nucleotides were locked in place after hybridization. This provided greater stability as an increase in the melting temperature of the hybridized complex[33].

As illustrated in figure 4, mir-196a can be clearly discriminated from mir-196b and mir-149. Compared to mir-196a, mir-196b with a mismatch nucleotide showed detection signal (8.7%). While the signal detected from sample matrices that contained 1) both mir-196a and mir-196b, and 2) mir-196a, mir-196b, and mir-149 was 108 % and 99 % respectively. It elucidated that LNA detection probe exhibits a high specificity to the complementary target.

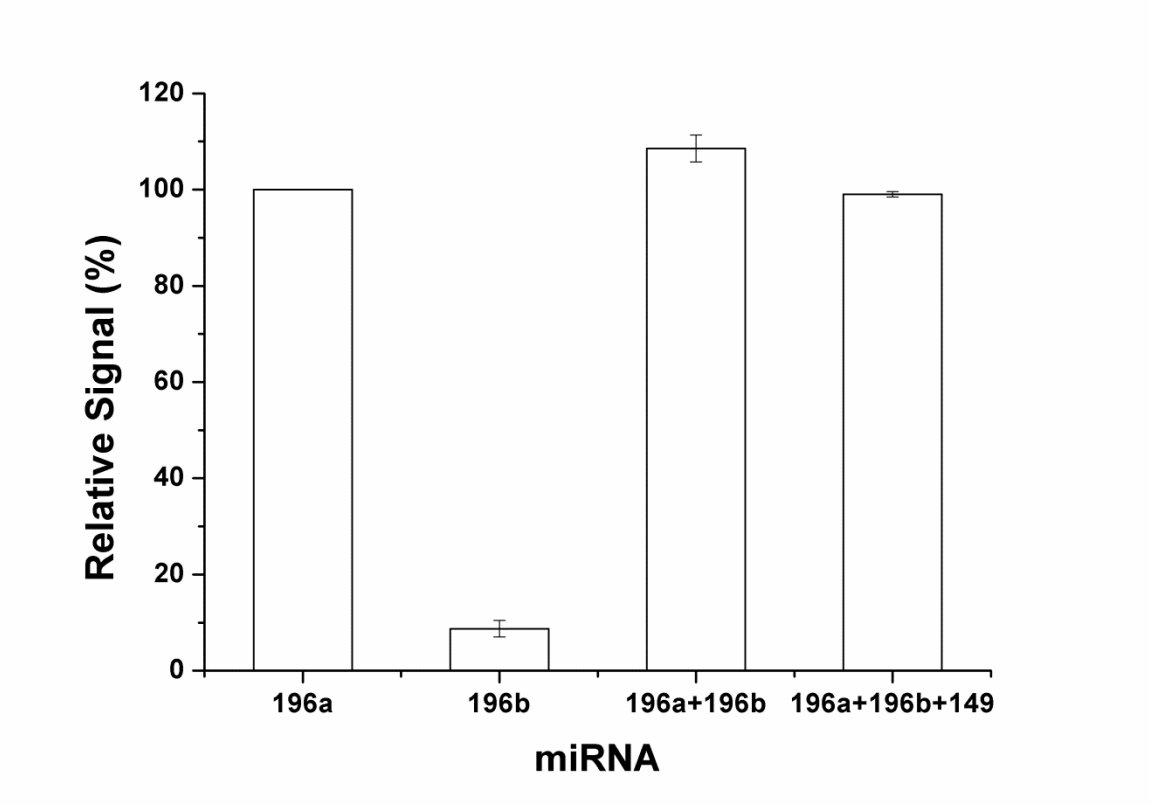

Figure 4. Study on the single-base mismatch discrimination efficiency (%) of the assay. The relative signal produced by mir-196a is normalized to 100%, the relative detection of the other miRNAs are calculated by the correlation equation in figure 3. The concentration of each miRNAs is 50 pM. The detection platform shows high specificity towards the target analyte, and is able to discriminate sample which deviated by a single-base mismatch. Error bars, standard error of mean, n = 3.

3.4 Quantification of mir-196a in normal and cancer patient's serum samples. We then applied the developed assay to quantify the expression of mir-196a in both normal and NPC cancerous serum samples. Since the fluorescent dye YOYO-1 has no selectivity towards oligonucleotides like mRNA, tRNA and other kind of small RNAs in such a complex sample matrix, in order to eliminate the unwanted signal from the background matrixes, standard addition method was applied in a manner that total synthetic target miRNA (mir-196a) was spiked into mixture of probes and the serum samples without any sample pre-treatment to the serum. The concentration of the mir-196a in the serum samples was obtained by extrapolation of the calibration curve. Two independent calibration curves were prepared for the two serum samples and the concentration mir-196a in each serum sample was determined. Both calibration curves showed good correlation between the concentration of the mir-196a and the intensity of the fibril with coefficient of determination above 0.989 (Figure 5). The content of mir-196a in normal and cancerous serum samples were estimated to be 7.9 ± 0.2 pM and 13.5 ± 0.3 pM respectively. The original concentration of mir-196a was then corrected by 5-fold dilution factor to be 40 and 68 pM. The result agreed with literature report that mir-196a is the up-regulated in nasopharyngeal carcinoma[34]. While the entire assay could be completed within 2 hrs, which is fast compared to traditional qRT-PRC, a direct quantification with minute sample consumption (~ 5 μL) was achieved. It is promising for constructing miRNA expression profile in real sample.

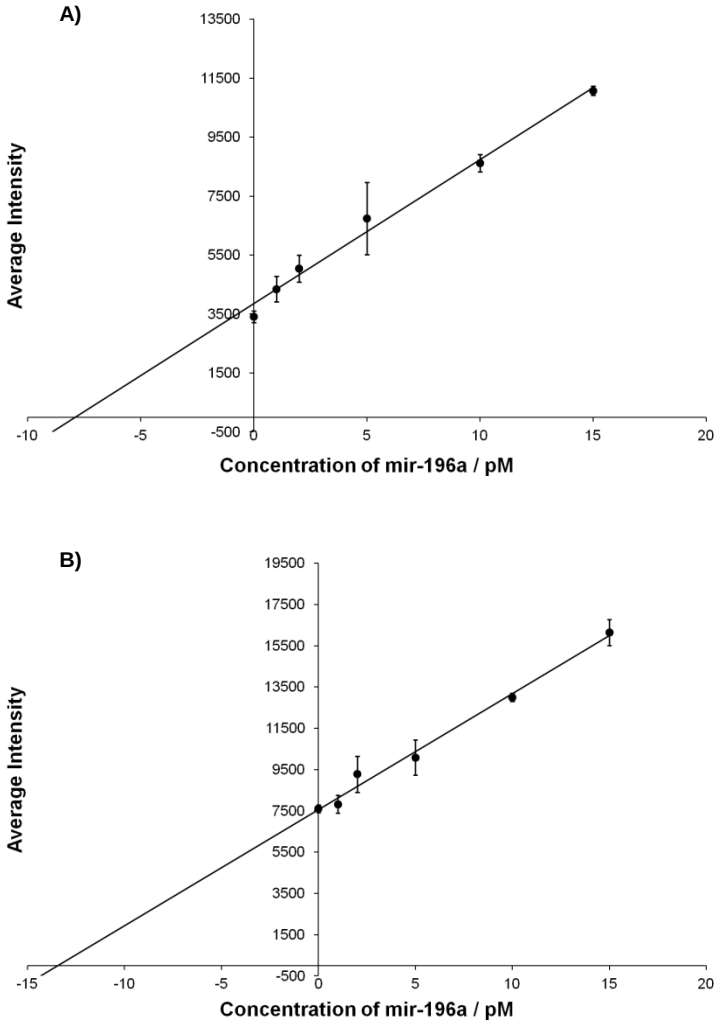

Figure 5. Quantification of mir-196a in (A) normal serum and (B) cancer patient's serum samples by standard addition method. Synthetic mir-196a was spiked into the serum samples. Error bars, standard error of mean, n = 3.

4. Conclusion

In this work, we developed a sensitive and specific platform for quantification of miRNAs. As a proof-of-concept, the concentration of mir-196a was quantified in both normal and cancerous serum samples. Profiling of these small regulatory miRNAs provides valuable information to diagnostics test developers as well as pharmaceutical companies. The protein-based detection assay can be readily modified and applied in immunoassays, in which the probe sequence on the fibrillar sensor can be converted from oligonucleotide probes into antibodies for capturing disease-related antigens or other acceptor molecules. Similarly, the LNA probes are also readily replaced by ATP aptamer, cardiac disease markers, thrombin aptamer, tumor angiogenesis markers, etc., for academic, biomedical researches and many other clinical applications.

ACKNOWLEDGEMENTS

This work is supported by the Young Scientists Fund from the National Science Foundation of China (21205006), and the University Grants Council of Hong Kong Special Administrative Region, China (GRF/HKBU201612, AoE/M06/08), and Faculty Research Grant of Hong Kong Baptist University (FRG2/11-12/126).

References:

1. de Planell-Saguer, M.; Rodicio, M. C. Analytical aspects of microRNA in diagnostics: A review. *Anal. Chim. Acta* **2011,** *699* (2), 134-152.
2. Kwak, P. B.; Iwasaki, S.; Tomari, Y. The microRNA pathway and cancer. *Cancer Sci.* **2010,** *101* (11), 2309-2315.
3. Pritchard, C. C.; Cheng, H. H.; Tewari, M. MicroRNA profiling: approaches and considerations. *Nat. Rev. Genet.* **2012,** *13* (5), 358-369.
4. Bartel, D. P. MicroRNAs: Genomics, biogenesis, mechanism, and function. *Cell* **2004,** *116* (2), 281-297.
5. Esquela-Kerscher, A.; Slack, F. J. Oncomirs - microRNAs with a role in cancer. *Nat. Rev. Cancer* **2006,** *6* (4), 259-269.
6. Chen, X.; Ba, Y.; Ma, L. J.; Cai, X.; Yin, Y.; Wang, K. H.; Guo, J. G.; Zhang, Y. J.; Chen, J. N.; Guo, X.; Li, Q. B.; Li, X. Y.; Wang, W. J.; Zhang, Y.; Wang, J.; Jiang, X. Y.; Xiang, Y.; Xu, C.; Zheng, P. P.; Zhang, J. B.; Li, R. Q.; Zhang, H. J.; Shang, X. B.; Gong, T.; Ning, G.; Wang, J.; Zen, K.; Zhang, J. F.; Zhang, C. Y. Characterization of microRNAs in serum: a novel class of biomarkers for diagnosis of cancer and other diseases. *Cell Res.* **2008,** *18* (10), 997-1006.
7. Wark, A. W.; Lee, H. J.; Corn, R. M. Multiplexed detection methods for profiling microRNA expression in biological samples. *Angew. Chem.-Int. Edit.* **2008,** *47* (4), 644-652.
8. Lin, S. L.; Chang, D.; Ying, S. Y. Asymmetry of intronic pre-miRNA structures in functional RISC assembly. *Gene* **2005,** *356*, 32-38.
9. Tian, T.; Xiao, H.; Zhang, X. L.; Peng, S.; Zhang, X. E.; Guo, S.; Wang, S. R.; Liu, S. M.; Zhou, X.; Meyers, C.; Zhou, X. Simultaneously sensitive detection of multiple miRNAs based on a strand displacement amplification. *Chem. Commun.* **2012,** *49* (1), 75-77.
10. Bustin, S. A.; Mueller, R. Real-time reverse transcription PCR (qRT-PCR) and its potential use in clinical diagnosis. *Clin. Sci.* **2005,** *109* (4), 365-379.
11. Valoczi, A.; Hornyik, C.; Varga, N.; Burgyan, J.; Kauppinen, S.; Havelda, Z. Sensitive and specific detection of microRNAs by northern blot analysis using LNA-modified oligonucleotide probes. *Nucleic Acids Res.* **2004,** *32* (22).
12. Lim, L. P.; Lau, N. C.; Garrett-Engele, P.; Grimson, A.; Schelter, J. M.; Castle, J.; Bartel, D. P.; Linsley, P. S.; Johnson, J. M. Microarray analysis shows that some microRNAs downregulate large numbers of target mRNAs. *Nature* **2005,** *433* (7027), 769-773.
13. Kilic, T.; Topkaya, S. N.; Ariksoysal, D. O.; Ozsoz, M.; Ballar, P.; Erac, Y.; Gozen, O. Electrochemical based detection of microRNA, mir21 in breast cancer cells. *Biosens. Bioelectron.* **2012,** *38* (1), 195-201.
14. Wu, X. Y.; Chai, Y. Q.; Yuan, R.; Su, H. L.; Han, J. A novel label-free electrochemical microRNA biosensor using Pd nanoparticles as enhancer and linker. *Analyst* **2013,** *138* (4), 1060-1066.
15. Li, C. P.; Li, Z. P.; Jia, H. X.; Yan, J. L. One-step ultrasensitive detection of microRNAs with loop-mediated isothermal amplification (LAMP). *Chem. Commun.* **2011,** *47* (9), 2595-2597.
16. Yin, B. C.; Liu, Y. Q.; Ye, B. C. One-Step, Multiplexed Fluorescence Detection of microRNAs Based on Duplex-Specific Nuclease Signal Amplification. *J. Am. Chem. Soc.* **2012,** *134* (11), 5064-5067.
17. Chan, H. M.; Chan, L. S.; Wong, R. N. S.; Li, H. W. Direct Quantification of Single-Molecules of MicroRNA by Total Internal Reflection Fluorescence Microscopy. *Anal. Chem.* **2010,** *82* (16), 6911-6918.
18. Alhasan, A. H.; Kim, D. Y.; Daniel, W. L.; Watson, E.; Meeks, J. J.; Thaxton, C. S.; Mirkin, C. A. Scanometric MicroRNA Array Profiling of Prostate Cancer Markers Using Spherical Nucleic Acid-Gold Nanoparticle Conjugates. *Anal. Chem.* **2012,** *84* (9), 4153-4160.

19. Weizmann, Y.; Chenoweth, D. M.; Swager, T. M. DNA-CNT Nanowire Networks for DNA Detection. *J. Am. Chem. Soc.* **2011** *133* (10), 3238-3241.
20. Zhang, G. J.; Chua, J. H.; Chee, R. E.; Agarwal, A.; Wong, S. M. Label-free direct detection of MiRNAs with silicon nanowire biosensors. *Biosens. Bioelectron.* **2009,** *24* (8), 2504-2508.
21. Dong, H. F.; Lei, J. P.; Ju, H. X.; Zhi, F.; Wang, H.; Guo, W. J.; Zhu, Z.; Yan, F. Target-Cell-Specific Delivery, Imaging, and Detection of Intracellular MicroRNA with a Multifunctional SnO2 Nanoprobe. *Angew. Chem.-Int. Edit.* **2012,** *51* (19), 4607-4612.
22. Gao, X. Y.; Matsui, H. Peptide-based nanotubes and their applications in bionanotechnology. *Adv. Mater.* **2005,** *17* (17), 2037-2050.
23. Chan, H. M.; Li, H. W. Multifunctional Encoded Self-Assembling Protein Nanofibrils as Platform for High-Throughput and Multiplexed Detection of Biomolecules. *Anal. Chem.* **2011,** *83* (24), 9370-9377.
24. Pereira, P. M.; Marques, J. P.; Soares, A. R.; Carreto, L.; Santos, M. A. S. MicroRNA Expression Variability in Human Cervical Tissues. *PLoS One* **2010,** *5* (7).
25. Niinuma, T.; Suzuki, H.; Nojima, M.; Nosho, K.; Yamamoto, H.; Takamaru, H.; Yamamoto, E.; Maruyama, R.; Nobuoka, T.; Miyazaki, Y.; Nishida, T.; Bamba, T.; Kanda, T.; Ajioka, Y.; Taguchi, T.; Okahara, S.; Takahashi, H.; Nishida, Y.; Hosokawa, M.; Hasegawa, T.; Tokino, T.; Hirata, K.; Imai, K.; Toyota, M.; Shinomura, Y. Upregulation of miR-196a and HOTAIR Drive Malignant Character in Gastrointestinal Stromal Tumors. *Cancer Res.* **2012,** *72* (5), 1126-1136.
26. Szafranska, A. E.; Davison, T. S.; John, J.; Cannon, T.; Sipos, B.; Maghnouj, A.; Labourier, E.; Hahn, S. A. MicroRNA expression alterations are linked to tumorigenesis and non-neoplastic processes in pancreatic ductal adenocarcinoma. *Oncogene* **2007,** *26* (30), 4442-4452.
27. Chan, H. M.; Xiao, L. H.; Yeung, K. M.; Ho, S. L.; Zhao, D.; Chan, W. H.; Li, H. W. Effect of surface-functionalized nanoparticles on the elongation phase of beta-amyloid (1-40) fibrillogenesis. *Biomaterials* **2012,** *33* (18), 4443-4450.
28. Man, B. Y. W.; Chan, H. M.; Leung, C. H.; Chan, D. S. H.; Bai, L. P.; Jiang, Z. H.; Li, H. W.; Ma, D. L. Group 9 metal-based inhibitors of beta-amyloid (1-40) fibrillation as potential therapeutic agents for Alzheimer's disease. *Chem. Sci.* **2011,** *2* (5), 917-921.
29. Yang, W. G.; Wong, Y.; Ng, O. T. W.; Bai, L. P.; Kwong, D. W. J.; Ke, Y.; Jiang, Z. H.; Li, H. W.; Yung, K. K. L.; Wong, M. S. Inhibition of Beta-Amyloid Peptide Aggregation by Multifunctional Carbazole-Based Fluorophores. *Angew. Chem.-Int. Edit.* **2012,** *51* (8), 1804-1810.
30. Xia, T. B.; SantaLucia, J.; Burkard, M. E.; Kierzek, R.; Schroeder, S. J.; Jiao, X. Q.; Cox, C.; Turner, D. H. Thermodynamic parameters for an expanded nearest-neighbor model for formation of RNA duplexes with Watson-Crick base pairs. *Biochemistry* **1998,** *37* (42), 14719-14735.
31. Cosa, G.; Focsaneanu, K. S.; McLean, J. R. N.; McNamee, J. P.; Scaiano, J. C. Photophysical properties of fluorescent DNA-dyes bound to single- and double-stranded DNA in aqueous buffered solution. *Photochem. Photobiol.* **2001,** *73* (6), 585-599.
32. Luo, Z. H.; Zhang, L. Y.; Li, Z.; Li, X. Y.; Li, G.; Yu, H. B.; Jiang, C.; Dai, Y. F.; Guo, X. F.; Xiang, J. J.; Li, G. Y. An in silico analysis of dynamic changes in microRNA expression profiles in stepwise development of nasopharyngeal carcinoma. *BMC Med. Genomics* **2012,** *5*.
33. Nuovo, G. J. In situ detection of microRNAs in paraffin embedded, formalin fixed tissues and the co-localization of their putative targets. *Methods* **2010,** *52* (4), 307-315.
34. TANG, S.-y.; HUANG, G.-l.; LU, Y.; HE, Z.-w. Relationship between hsa-mir-196a-2 gene polymorphism and susceptibility and clinicopathologic factors of nasopharyngeal carcinoma in Hunan Han people. *Journal of Guangdong Medical College* **2013** (1), 8-10,14.